Reliability-Driven Deployment in Energy-Harvesting Sensor Networks

Xiaofan Yu*, Xueyang Song*, Ludmila Cherkasova† and Tajana Šimunić Rosing*
*Department of Computer Science and Engineering
University of California San Diego, La Jolla, USA
Email: {x1yu, xus023, tajana}@ucsd.edu
†Arm Research, San Jose, USA
Email: ludmila.cherkasova@arm.com

***Abstract*—Recent years have witnessed a significant expansion in Internet-of-Things (IoT) applications, especially in environmental monitoring, which aims at providing full coverage over potential targets. With energy harvesting ability, sensor devices can be replenished by external energy sources, and thus their lifetime is prolonged. While existing literature focuses on minimizing deployment cost, the reliability management is overlooked. Previous research has addressed that a higher temperature exponentially accelerates hardware failure rates. The versatile outdoor environments impose a non-negligible thermal stress on the hardware and consequently reduce the reliability of devices. In this paper, we are the first to propose a reliability-driven sensor deployment approach to achieve minimum nodes, while satisfying (i) full target coverage, (ii) complete connectivity, (iii) energy-neutral operation, and (iv) reliability constraints. Given external temperature distribution, we propose an algorithm to convert reliability constraints to a single-value power threshold for each location. A Mixed Integer Linear Programming (MILP) model is formulated and solved with CPLEX. Due to the complex nature of MILP, we propose a heuristic, named Reliability-driven Two-Stage Heuristic (R-TSH), to approximate the optimal solution for large-scale problems. Extensive simulations are performed on a real-world dataset from the National Solar Radiation Database. Our results indicate that R-TSH meets all reliability constraints with only 20% more sensors than the optimal solution, while executing more than 1500x faster. Compared to state-of-the-art heuristics, R-TSH avoids 20 - 80% of reliability violations with a comparable number of nodes and execution time.**

***Index Terms*—IoT Networks, Sensor Deployment, Reliability.**

I. Introduction

The rise of ubiquitous computing and Internet-of-Things (IoT) network has encouraged numerous environmental monitoring applications, e.g., Smart City [1], Smart Agriculture [2]. According to Ericsson's report, around 1.5 billion IoT devices with cellular connections will be spread over the globe in 2022 [3]. A common goal of these applications is to fully cover point-of-interests (PoIs) or areas with sensor networks, while achieving less cost or longer lifetime under careful management [4], [5]. Energy harvesting techniques can further extend the lifetime of devices. With rechargeable batteries, refilled by external sources such as solar radiation, sensor devices ideally may obtain infinite lifetime if their energy consumption is less than the harvested energy. This usage mode is called *energy-neutral operation* [6].

Device placement, being the first step in establishing the IoT network design, makes a significant impact on the IoT network reliability and its lifespan. Common management techniques such as resource allocation, load balancing, and flow management can improve the Quality-of-Service and lifetime of an established network [7], [8], but device placement decisions set the upper bound on such improvements. Using optimization to determine the node placement appears as a common method in designing the traditional content delivery networks [9], where the goal is to carefully place replica servers to minimize service latency. In contrast, sensor placement for ubiquitous IoT networks is different since versatile environmental conditions such as temperature and solar radiation need to be considered.

Existing works in energy-harvesting sensor networks deployment have studied minimizing deployment cost after ensuring: (i) coverage (i.e., all PoIs are covered), (ii) connectivity (i.e., all devices are directly or indirectly connected to the gateway), and (iii) energy-neutral operation [10], [11]. However, the reliability factors are overlooked in the previous work. Even with infinite energy income, both storage and computing subsystems degrade over time and ultimately require repairing or complete replacement. State-of-the-art electronics aging models revealed that the failure rates of hardware systems depend exponentially on temperature [12]. More concretely, the mean-time-to-failure (MTTF, i.e., the expected time to failure) of a device is exponentially shortened under high temperatures. The capacity and power output of batteries also degrade exponentially faster in hot environments, whose aging status is described by the State of Health (SoH) [13]. Starting from $SoH = 1$, a battery reaches its end of life when SoH decreases to 0.8 regardless of the remaining charge [14]. If not managed carefully, the expenditure on maintenance can take up to 80% of the total deployment cost. As reported by Cisco [15], $3.2M/year will be spent in administrative labor and technical support due to system failures for every 100K devices. Reliability will become the major bottleneck in the future IoT deployment, especially for outdoor environmental monitoring under extreme temperatures.

In this paper, we study the methods to manage the reliability of an energy-harvesting sensor network from the very first step of deployment. The contributions are four-fold:

- We are the first to attack the problem of reliability-driven energy-harvesting sensor deployment for environmental monitoring. We integrate the state-of-the-art reliability models of electronics and battery state-of-health, both of which exponentially rely on temperature.
- We formulate an optimization problem minimizing the number of nodes, while achieving (i) full coverage on

PoIs, (ii) complete connectivity, (iii) energy-neutral operation, and (iv) reliability constraints. The formulated problem is a Mixed Integer Linear Program (MILP), which is solved by CPLEX. We proved that the proposed problem is NP-complete.
- We offer a greedy heuristic named Reliability-driven Two-Stage Heuristic (R-TSH) in search of suboptimal solutions in large-scale problems.
- Extensive simulations are conducted based on a real-world solar irradiance and ambient temperature dataset from the National Solar Radiation Database (NSRDB) [16]. Our results show that R-TSH meets all reliability constraints with 20% more sensors than the optimal solution while executing more than 1500x faster. Compared with previous heuristics, R-TSH avoids 20 - 80% of reliability violations with a comparable number of nodes and execution time.

The rest of the paper is organized as follows: Section II summarizes related literature. Section III introduces the background of reliability models used in the paper. The optimization problem is formulated and solved in Section IV. Section V explicitly describes the design of R-TSH. Evaluation setup and results are discussed in Section VI. Finally, the whole paper concludes in Section VII.

II. Related Work

A. Sensor Deployment in Wireless Sensor Networks

Existing literature on sensor deployment mainly optimizes coverage [17], connectivity [18], and network lifetime [19]. In terms of coverage, application requirements can be categorized into area coverage, target coverage, and barrier coverage [5]. The optimization goal is designing a network with minimum deployment cost or longest lifetime while satisfying the coverage and connectivity requirements [4]. To find the optimal solution, grid placement is transformed into integer programming models and solved with conventional solvers. However, NP-hardness of integer programming problems results in poor scalability, and therefore encourages the development of efficient heuristics to approximate the optimum within finite time [17], [18], [20]. All the above-mentioned works assume single-use batteries, so the network lifetime is limited.

In recent years, renewable energy has opened up novel possibilities in sensor deployment. With energy harvesting, a sensor node can operate perpetually if placed at a location with sufficient energy input. Yang *et al.* [10] is the first to formulate a sensor placement problem for achieving energy-neutral operation with the goal of covering fixed targets and ensuring connectivity to the gateway. Along with bringing out a Mixed Integer Linear Programming (MILP) problem, the authors proposed two greedy heuristics that require 20% and 10% more sensors than MILP in the simulation. The later work by Zhu *et al.* [11] considers the placement of directional energy-harvesting sensors for target coverage. They also consider solar panel size at each site as variables which determine the energy-harvesting rate. Three heuristics were offered, along with the corresponding analyses on time complexity and performance bound. Nevertheless, neither of [10] or [11] considered reliability, which causes striking differences in versatile outdoor environments.

B. Reliability-Driven Network Deployment

Reliability has become increasingly important for large-scale networks that may introduce enormous maintenance costs. For traditional data-center networks, the common strategy to improve reliability is duplicating network service on replica servers, so that latency requirements are met even if some servers are down [9], [21]. While sensor networks present more uncertainties on device- and communication-level, previous works applied similar ideas of placing redundant nodes to enhance the fault tolerance of the network. Extra nodes can be placed to achieve *k-coverage* (i.e., any point of interest (PoI) needs to be covered by at least k sensors), which ensures reliable sensing since failures of less than k nodes will not hinder a successful detection [19]. A similar *m-connectivity* constraint (i.e., any sensor is required to have m distinct paths to the gateway) can guarantee reliable data transmission when unexpected link failures occur [22]. All the above-mentioned contributions are able to temporarily mitigate the negative influence on network functionality upon failures.

However, very few existing papers offer the models of failure mechanisms/conditions and address how to preventively reduce the failure rates. On this track, the most recent work by Yu *et al.* [23] studied temperature-based sensor deployment for the minimal maintenance cost considering single-use battery depletion and electronics failures. A non-convex nonlinear optimization problem is formulated and approximated with metaheuristics. Simulation results demonstrated that their strategy can save up to 40% of maintenance cost compared to existing greedy heuristics. Although concrete failure mechanisms are modeled, their methodology is not applicable to energy-harvesting sensor networks where rechargeable batteries are used. In this paper, we approach the problem differently from [23] by assuming the following:

- We consider more commonly-applied grid deployment for target coverage rather than continuous-space monitoring.
- We introduce electronics MTTF and battery SoH constraints, the latter of which focus on rechargeable batteries instead of the single-use ones.

III. Background on Reliability

Reliability of a system is a probability function $R(t)$ defined on $[0, \infty]$ that the system will not fail until time t [12]. It is highly related to the failure rate of a system, which shows a bathtub curve as a function of time [24]. While failure rates in the initial burn-in and final wear-out periods of a system change rapidly, we focus on the useful lifetime of systems during which the failure rates are constant. Failures in sensor networks can be categorized into link failures, software failures, and hardware failures [25]. We recognize that both link and software failures can be recovered or avoided if designed properly. For example, a software issue can be resolved by updating firmware remotely. In this paper, we mainly consider permanent hardware failures which require significant maintenance effort including device repair or complete replacement. Specifically, we use state-of-the-art reliability models for two key components of sensor networks: electronics and battery, stressing the impact of ambient temperature.

A. Electronics Reliability Model

Previous research has studied common electronics failure mechanisms including time-dependent dielectric breakdown, negative bias temperature instability, electromigration, and thermal cycling, all of which are accelerated exponentially by the core temperature [12], [26]. We use the term *core temperature* to refer to the internal temperature of a chip. The MTTF for each mechanism can be modeled as a function of time, voltage, temperature, and technological parameters. In [24], the authors showed that the MTTF of all above-mentioned mechanisms share a similar form depending on the core temperature T_c. We extract this general expression to estimate MTTF as the ratio to the standard case under $T_{ref} = 25$°C:

$$MTTF(T_c) = \exp(\frac{E_a}{kT_c}) / \exp(\frac{E_a}{kT_{ref}}), \tag{1}$$

where E_a is the activation energy, k is Boltzmann's constant. According to the thermal dissipation model in [27], T_c linearly depends on average power consumption P of the device and ambient temperature T_{amb} at the deployed location:

$$T_c = k_1 P + k_2 T_{amb} + k_3. \tag{2}$$

where k_1, k_2 and k_3 are device-specific parameters obtained by fitting into experimental traces.

B. Battery Reliability Model

In contrast to the state-of-charge model that predicts the available charge in a battery, we utilize the state-of-health model denoting a battery's aging level in comparison to its brand new state. Even though a battery can be recharged by harvested energy, it suffers from capacity and power fade which eventually makes the battery unusable. The operational lifetime of a battery is defined as the time when SoH reduces from 1 to 0.8 [14]. It is widely recognized that battery aging consists of calendar aging and cycle aging [28]. While calendar aging is exponentially accelerated by time, temperature, and state-of-charge stresses, cycle aging additionally accounts for the degradation due to the depth of discharge (DoD) in each charge-discharge cycle. We use the state-of-the-art semi-empirical SoH model in [14] for Lithium-Ion batteries. Since our goal is to optimize long-term state-of-health, we mainly focus on calendar aging with time and temperature stresses:

$$SoH(t, T_{cell}) = \exp\left\{-k_t t \exp\left[k_T T_{ref}\left(1 - \frac{T_{ref}}{T_{cell}}\right)\right]\right\}. \tag{3}$$

Here t is the elapsed time. T_{cell} is the internal battery cell temperature and T_{ref} is the reference temperature of 25 °C. k_t and k_T are predetermined constants. Similar to estimating core temperature, we employ the thermal model in [27] to convert ambient temperature T_{amb} to battery cell temperature T_{cell} with different linear coefficients.

IV. Optimal Problem Formulation

In this section, we explain the formulation of the optimal sensor deployment problem and how to solve it. We consider deploying sensor nodes into a grid candidate space N to cover a set of PoIs denoted by O. For ease of reading, we list the important symbols used in our formulation in Table I. Assuming at most one device can be placed at a grid point and only one gateway exists, the optimization problem minimizes the number of deployed nodes subject to the following constraints:

- K-*coverage*. Each PoI is covered by at least K sensors.
- *Complete connectivity*. All generated data can be successfully routed to the gateway.
- *Energy-neutral operation*. At each deployed site, the energy consumption is less than the harvested energy.
- *Reliability constraints*. Using the models in Section III, the reliability of each deployed device after a predetermined time duration $Time$ is greater than a given bound.

TABLE I: List of important notations in problem formulation.

Symbol	Meaning
N	Set of grid locations
O	Set of point-of-interests
S_r	Feasible sensing radius
C_r	Feasible communication radius
K	Required coverage level
G	Quantity of data in each sample
γ	The maximum possible flow amount
η	Uniform sampling frequency
BW	Communication bandwidth
d_{ij}	Euclidean distance between grid locations i and j
Γ_i, Γ_B	Set of neighbor nodes of node i and the gateway
x_i	Binary variable of whether a device is placed at i
s_i	Binary variable of whether a sensor is placed at i
f_{ij}, f_{iB}	Average flow quantity from i to j and to the gateway
P_{tx}, P_{rx}	Average transmission and reception power
P_i	Average power consumption rate at node i
$P_{SoH,i}$	Power upper bound to meet SoH lower bound at i
$P_{MTTF,i}$	Power upper bound to meet MTTF lower bound at i
R_i	Energy harvesting rate at node i
$T_{amb,i}$	Ambient temperature at node i
$T_{cell,i}$	Battery cell temperature at i
$T_{c,i}$	Internal core temperature at i
T_{ref}	Reference temperature of 25 °C
$Time$	Elapsed time for reliability evaluation

The binary variables of the problem are x_i (Equation 4) and s_i (Equation 5). While x_i suggests whether a device is placed at location i, s_i further indicates whether the device performs sensing actions. x_i and s_i enable the problem to distinguish relay nodes (i.e., nodes that only route data) and sensor nodes (i.e., nodes that carry out both sensing and transmission). The continuous variables are f_{ij} and f_{iB} while representing the flow quantity from node i to j and from node i to the gateway respectively.

$$x_i = \begin{cases} 1 & \text{if a device is placed at } i \\ 0 & \text{otherwise.} \end{cases} \tag{4}$$

$$s_i = \begin{cases} 1 & \text{if a sensor is placed at } i \\ 0 & \text{otherwise.} \end{cases} \tag{5}$$

To help the readers get familiar with the notations, we depict an example deployment in Figure 1. Each grid point is viewed as a candidate site. The red triangles represent deployed sensor nodes ($x_i = 1, s_i = 1$) whose sensing radius is shown by the red circle. Both PoIs (green diamonds) are successfully covered by the deployed sensors with level $K = 1$. Differently, the blue dots denote for pure relay nodes ($x_i = 1, s_i = 0$) that only route data. All nodes are connected to the gateway (orange star).

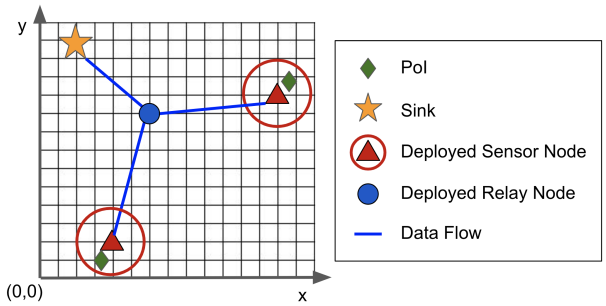

Fig. 1: An example deployment instance.

Now we rigorously formulate the problem as MILP with the following mathematical form:

$$\min \sum_{i \in N} x_i \tag{6}$$

subject to

$$\sum_{i \in N} s_i \cdot cov(i,j) \geq K, \quad \forall j \in O \tag{7a}$$

$$s_i \eta G + \sum_{j \in \Gamma_i} f_{ji} = \sum_{j \in \Gamma_i} f_{ij} + f_{iB}, \quad \forall i \in N \tag{7b}$$

$$\sum_{i \in \Gamma_B} f_{iB} = \sum_{i \in N} s_i \eta G \tag{7c}$$

$$s_i \leq x_i, \quad \forall i \in N \tag{7d}$$

$$\sum_{j \in \Gamma_i} f_{ij} \leq \gamma x_i, \quad \forall i \in N \tag{7e}$$

$$P_i = P_0 + s_i E_s \eta + \sum_{j \in \Gamma_i} \left(P_{tx}(d_{ij}) \frac{f_{ij}}{BW} + P_{rx} \frac{f_{ji}}{BW} \right), \ \forall i \in N \tag{7f}$$

$$P_i \leq \min \{R_i, P_{SoH,i}, P_{MTTF,i}\}, \quad \forall i \in N \tag{7g}$$

$$x_i \in \{0,1\}, s_i \in \{0,1\}, \quad \forall i \in N \tag{7h}$$

$$0 \leq f_{ij} \leq \gamma, \quad \forall i \in N, j \in N, i \neq j \tag{7i}$$

Equation 7a is the *K-coverage* constraint. Equation 7b and 7c impose the connectivity requirements. Specifically, Equation 7b requires the sum of generated data and incoming flows to be equal to the total quantity of outgoing flows. Equation 7c guarantees all sensed data are converged at the gateway. Equation 7d and 7e are feasibility constraints. The former equation states a sensor can only be placed at the site where a device exists, while the latter one claims no flow can pass through node i if no device is located there. $\gamma = \eta G |N|$ is defined as the maximum possible flow quantity in the network. Equation 7f illustrates the linear power model, after which Equation 7g ensures that energy-neutral operation and reliability constraints are achieved at each site. Last but not least, Equation 7h and 7i give the lower and upper limits for all variables. We concretize and explain each constraint in the following lines.

Coverage Constraint: We employ the fundamental binary coverage model as follows [4]:

$$cov(i,j) = \begin{cases} 1 & \text{if } d(i,j) < S_r, \\ 0 & \text{otherwise.} \end{cases} \tag{8}$$

S_r denotes for the feasible sensing radius. $d(i,j)$ reports the Euclidean distance between $i \in N$ and $j \in O$. Adopting the *K-coverage* concept [19], a full coverage in our formulation means each target is supervised by as least K sensors:

$$\sum_{i \in N} s_i \cdot cov(i,j) \geq K \quad \forall j \in O \tag{9}$$

Connectivity Constraint: We assume the feasible communication range of each device to be C_r. Then the neighbor set Γ_i of grid node i is defined as $\Gamma_i = \{j \in N \mid d_{ij} < C_r, j \neq i\}$, where d_{ij} denotes the Euclidean distance between grid locations i and j. Similarly, Γ_B represents the set of neighbor nodes of the gateway. The connectivity constraints require: (i) flow conservation, i.e., the sum of the outgoing flow should equal to the sum of the incoming flow and generated data (if any) at each node (Equation 7b), (ii) complete connectivity, i.e., all data generated from end devices converge into the gateway (Equation 7c).

Energy-Neutral Operation Constraint: To achieve energy-neutral operation at each deployed spot, we require the average power of the device is less than or equal to the harvesting rate. The power of an energy-harvesting sensor node can be classified into ambient power (e.g. dissipated power during the sleep state), sensing power, and communication power [29]. We assume the system is woken up once in a sampling interval T_{cycle}, performs the sensing task, transmits the packet, and is set to sleep again before the next cycle. We utilize the following equation to model the average power of a device at grid location i:

$$P_i = P_0 + s_i E_s \eta + \sum_{j \in \Gamma_i} \left(P_{tx}(d_{ij}) \frac{f_{ij}}{BW} + P_{rx} \frac{f_{ji}}{BW} \right) \tag{10}$$

where P_0 is a constant denoting the ambient power dissipation. E_s is the energy consumed per sensing task and $\eta = 1/T_{cycle}$ is the sampling frequency. Thus $E_s \eta$ stands for the average power in sensing. With s_i, sensing power is only counted when a sensor is placed at i. The last term in the bracket is the average transmission and reception power models from [30]. We apply a simplified version here using typical parameters for BPSK. The transmission power varies polynomially to the distance: $P_{tx}(d) = p_{to} + k \cdot d^{\alpha}$, where p_{to}, k, and α are predefined constants. On the other hand, the average reception power P_{rx} is configured as a fixed value. The continuous variables f_{ij} and f_{iB} denote for the average amount of flow from node i to node j and from node i to the gateway respectively. BW is the bandwidth of the link.

The average energy harvesting rate R_i at grid location i can be determined by the average solar irradiance level λ_i (W/m^2) [11]: $R_i = \xi A \lambda_i$, where ξ is the end-to-end conversion efficiency of the solar system, A is the surface area of the solar panel. Both ξ and A are constants in our formulation. λ_i is available from online databases such as NSRDB [16]. Now we are able to write the energy-neutral operation constraint at i as:

$$P_i \leq R_i \tag{11}$$

Reliability Constraints: With the models in Section III, we are able to estimate the reliability given ambient temperature and average power. Suppose the reliability status is evaluated

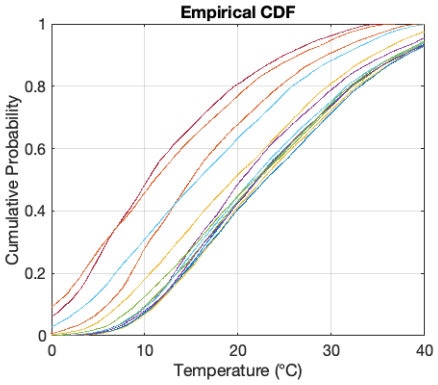

Fig. 2: The cumulative distribution of ambient temperature in one year at 10 equally-distributed locations in a 100 km $\times$ 100 km field in Southern California, US. The data is downloaded from NSRDB [16]. Each colored curve represents the temperature distribution over time at one of the locations.

after a predetermined time duration $Time$. Our goal is to decide a sensor deployment strategy such that certain reliability bounds can be met after $Time$ at each deployed location i. However, two issues are remaining unsolved.

Firstly, the ambient temperature T_{amb} changes over both time and space (Figure 2). Depending on the location, temperature can spread mostly in 10 - 40 °C (purple line) or in 0 - 30 °C region (red line). Consequently, at a fixed location, the SoH and MTTF can vary largely on the time horizon due to ambient temperature variations. We address this issue by taking an integral over the temperature distribution on the time axis. The expectation of SoH and $MTTF$ at a specific location i can be calculated as in Equation 12, where $p_{T_{amb,i}}$ is the probability associated with the temperature distribution at location i. Note, that the elapsed time for reliability evaluation is fixed to $Time$ and therefore is omitted from the variables.

$$\mathbb{E}\left[SoH(P_i)\right] = \int_{-\infty}^{\infty} SoH(T_{cell,i}(T_{amb,i}, P_i)) p_{T_{amb,i}} dT_{amb,i} \tag{12a}$$

$$\mathbb{E}\left[MTTF(P_i)\right] = \int_{-\infty}^{\infty} MTTF(T_{c,i}(T_{amb,i}, P_i)) p_{T_{amb,i}} dT_{amb,i} \tag{12b}$$

In practice, we can approximate Equation 12 by splitting the temperature distribution into sufficiently many bins and summing over all bins. Now the reliability constraints can be written as guaranteeing the expectation of SoH and MTTF to be greater than or equal to the predetermined bounds SoH_{ref} and $MTTF_{ref}$:

$$\mathbb{E}\left[SoH(T_{cell,i}(T_{amb,i}, P_i))\right] \geq SoH_{ref} \tag{13a}$$

$$\mathbb{E}\left[MTTF(T_{c,i}(T_{amb,i}, P_i))\right] \geq MTTF_{ref} \tag{13b}$$

The second issue is the nonlinearity of reliability models (Equation 1 and 3) which puts us in the complexities of solving a nonlinear optimization problem. *Is there a method to transform the nonlinear reliability constraints to linear inequalities?* To solve this issue, note that after the integral in Equation 12, the expectations of SoH and MTTF only rely on the average power of the device at location i. Specifically, given ambient temperature distribution, $\mathbb{E}\left[SoH\right]$ and $\mathbb{E}\left[MTTF\right]$ are monotones decreasing in P_i. Therefore we are able to reversely determine the corresponding upper bounds on average power to meet the reliability lower bounds. In this way, the nonlinear reliability constraints can be expressed as linear inequalities with previous linear power models. We employ the binary search algorithm to efficiently estimate the power upper bound brought by SoH and MTTF constraints (i.e., $P_{SoH,i}$ and $P_{MTTF,i}$) within a precision of ε. Taking $P_{SoH,i}$ as an example, the complete procedure to convert reliability bounds to power bounds is written in Algorithm 1. Initiating the two ends of search space to 0 and P_{max}, Algorithm 1 takes at most $log_2(\lceil \frac{P_{max}}{\varepsilon} \rceil)$ iterations to locate the desired power bound.

Since both the energy-neutral operation and reliability constraints are expressed as power upper bounds, they can be combined into one single inequality as in Equation 7g:

$$P_i \leq \min\left\{R_i, P_{SoH,i}, P_{MTTF,i}\right\} \tag{14}$$

Algorithm 1 Converting State-of-Health Bound to Power Bound

Input: $SoH_{ref}, T_{amb,i}, \varepsilon$
Output: $P_{SoH,i}$
$P_{lb} \leftarrow 0$, $P_{ub} \leftarrow P_{max}$
while $P_{ub} - P_{lb} > \varepsilon$ **do**
  $P_{mid} \leftarrow (P_{ub} + P_{lb})/2$
  Update $\mathbb{E}\left[SoH(P_{mid})\right]$ as in Equation 12a
  if $\mathbb{E}\left[SoH(P_{mid})\right] = SoH_{ref}$ **then**
    return P_{mid}
  else if $\mathbb{E}\left[SoH(P_{mid})\right] > SoH_{ref}$ **then**
    $P_{lb} \leftarrow P_{mid}$ ▷ continue searching in higher-power zone
  else
    $P_{ub} \leftarrow P_{mid}$ ▷ continue searching in lower-power zone
  end if
end while
return $(P_{lb} + P_{ub})/2$

A. Problem Analysis

The number of decision variables in the formulated MILP is $2|N| + |N|^2$, where $2|N|$ of them are binary and the rest $|N|^2$ variables are continuous. After the simplification, we arrive at $|N|+1$ equality constraints and $3|N|+|O|$ inequality constraints. We implement and solve the proposed problem in CPLEX 12.10 [31]. However, by demonstrating the following theorem , we show that the proposed problem cannot be solved in polynomial time.

Theorem 1. *The proposed problem is NP-complete.*

Proof. By setting $G = 0, P_0 = 0, E_s = 0, P_{tx} = P_{rx} = 0, K = 1$, the original problem transforms to covering a given set of targets with minimum number of grid points, which is exactly the minimum set cover problem. Since the minimum set cover problem has been proved to be NP-complete [32], the proposed problem is also NP-complete. □

V. Proposed Heuristic: R-TSH

Given our optimization problem is NP-complete, we devise a greedy heuristic for large-scale problems. Based on the Two-State Heuristic (TSH) proposed in [11], we further include the reliability factors, leading to an algorithm named Reliability-driven Two-Stage Heuristic (R-TSH). The original TSH has two stages in sequence. The first stage greedily selects sensor nodes to achieve full coverage with minimum cost. Afterwards, the second stage concurrently finds the shortest communication path from each selected sensor to the gateway. While R-TSH also employs the two-stage mechanism, its optimization mechanism is quite different. Contrary to TSH that attempts to minimize the deployment cost, R-TSH makes selections based on the equivalent power bound $P_{bd,i} = \min\{R_i, P_{SoH,i}, P_{MTTF,i}\}$ at each site i. In this way, R-TSH guarantees both the energy-neutral operation and reliability targets with greedy choices.

Algorithm 2 shows the detailed implementation of R-TSH. The first sensor selection stage spans from line 1 to line 20. Here we greedily select the sensor locations with the maximum benefit:

$$Benefit_i = |S_i \cap U| \cdot P_{bd,i} \tag{15}$$

where S_i denotes the set of PoIs covered by location i and U represents the PoIs that have not been fully covered. The benefit function favors the locations contributing more to coverage while loose in power bounds. The selecting loop exits once the full K-coverage is attained, or no new coverage can be made. The latter case indicates that the problem is infeasible.

In the communication-path selection stage, we construct a directed graph by including all connectable edges and assign the following weight to edge (i, j) with tuned parameters ω_1, ω_2:

$$W(i,j) \leftarrow \omega_1 [i \in S] + \omega_2 \frac{(P_{tx}(d_{ij}) + P_{rx})\eta G/BW}{P_{bd,i} - (P_0 + E_s\eta [i \in S])} \tag{16}$$

Here the notation $[Cond]$ gives 1 when the inner condition *Cond* is met. The first term appends additional cost to the edge if i is not added in stage 1. The second term computes the ratio of increased transmission power and remaining power budget. Intuitively, the communication paths costing less transmission power and less critical in energy bounds as well as reliability constraints are given higher priorities. All selected sensor nodes and relay nodes are returned in X.

Algorithm 2 Reliability-driven Two-Stage Heuristic (R-TSH)

Input: $N, O, K, P_{bd,i}$
Output: X, S, F
1: $S \leftarrow \varnothing$
2: $U \leftarrow \{1, 2, ..., |O|\}$ ▷ PoIs not fully covered
3: $q_i \leftarrow K, \forall i \in N$ ▷ unsatisfied coverage requirements
4: **while** $U \neq \varnothing$ **do**
5: $S_i \leftarrow \sum_{j \in U} cov(i, j), \forall i \in N$ ▷ PoIs covered by i
6: $i^* \leftarrow \arg\max \{|S_i \cap U| \cdot P_{bd,i} \mid i \in N - S\}$
7: **if** $|S_{i^*} \cap U| = \varnothing$ **then**
8: **break** ▷ no new coverage
9: **end if**
10: **for all** $k \in |S_{i^*} \cap U|$ **do**
11: $q_k \leftarrow q_k - 1$
12: **if** $q_k \leq 0$ **then**
13: $U \leftarrow U - \{k\}$
14: **end if**
15: **end for**
16: $S \leftarrow S \cup \{i^*\}$
17: **end while**
18: **if** $U \neq \varnothing$ **then**
19: **return** Null ▷ infeasible in full coverage
20: **end if**
21: $V \leftarrow N$
22: $E \leftarrow \{(i, j) \mid i, j \in N, i \neq j, j \in \Gamma_i\}$
23: $W(i,j) \leftarrow \omega_1 [i \in S] + \omega_2 \frac{(P_{tx}(d_{ij}) + P_{rx})\eta G/BW}{P_{bd,i} - (P_0 + E_s\eta [i \in S])}, \forall (i, j) \in E$
24: Construct directed graph $GP(V, E, W)$
25: Concurrently find the shortest paths F from S to the gateway in GP using Dijkstra's algorithm.
26: $X \leftarrow \{i \mid i \in F\}$
27: **return** X, S, F

VI. Evaluation

A. Experimental Setup

We implement our problem and heuristic in MATLAB R2020a[1], while the MILP is solved by CPLEX 12.10 [31]. Simulation experiments are performed on a Linux desktop with Intel Core i7-8700 CPU at 3.2 GHz and 16 GB RAM. We use a dataset covering 100 km × 100 km region in Southern California, US, downloaded from NSRDB [16]. The dataset contains half-hourly solar irradiance and ambient temperature measurements of 836 locations from January 1, 2019, to January 1, 2020. To simulate deploying sensors onto various sizes of fields, we project the spatial temperature distribution to the candidate grid space. The positions of PoIs and the gateway are randomly initialized. We set the reliability bounds $SoH_{ref} = MTTF_{ref} = 0.9$ and elapsed time $Time = 3$ years. Table II reports the detailed parameter settings.

The performance of the following methods are evaluated:

- **OPT**: The optimal solution to the proposed problem.
- **OPT$_{\mathbf{noRel}}$**: The optimal solution to the proposed problem without reliability constraints.
- **R-TSH**: Our proposed heuristic.

We select two baselines from [11], TSH, and SRIGH to compare. Both TSH and SRIGH are devised to cover PoIs with minimum deployment cost while ensuring energy-neutral operation.

- **TSH**: The original two-stage heuristic in [11].
- **SRIGH**: Sensing- and routing- integrated greedy heuristic in [11]. SRIGH greedily selects a sensing node and its communication route within each iteration.

B. Results

1) Small-Scale Problem Simulation: First, we evaluate the performance of all methods on a small-scale problem. We create a grid space of 1000 m × 1000 m and set the desired coverage level to $K = 1$. The number of candidate grid sites is 100

[1]The source code is available at https://github.com/Orienfish/EH-deploy.

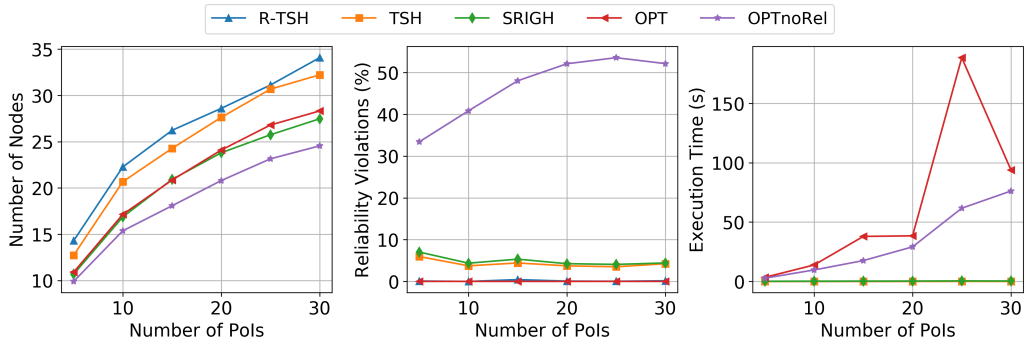

Fig. 3: Simulation results on a small field with various number of PoIs to cover. Left: the minimum deployed nodes. Middle: the percentage of reliability violations. Right: the execution time.

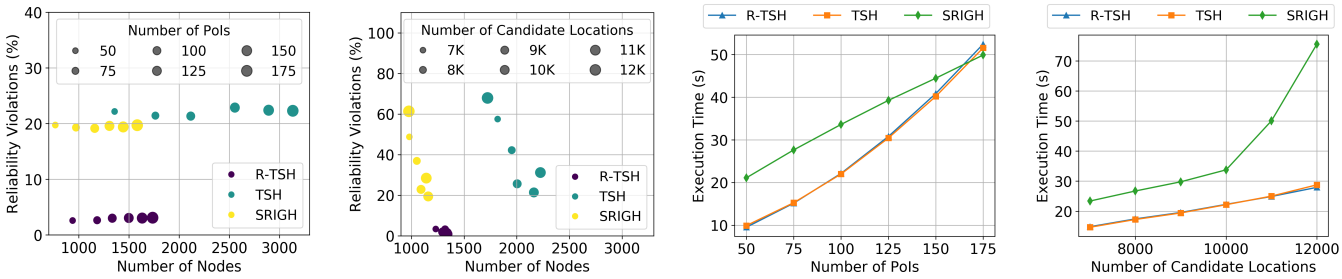

(a) Various number of PoIs.

(b) Various number of grid locations.

(c) Execution time when varying the number of PoIs.

(d) Execution time when varying the number of grid locations.

Fig. 4: Simulation results on a large field.

TABLE II: Parameter settings in evaluation.

Param.	Value	Param.	Value	Param.	Value
S_r	120 m	C_r	200 m	η	0.1
G	100 B	BW	2000 B/s	P_0	0.01 W
E_s	0.04 J	P_{to}	0.22 W	β	10^{-7}
α	3.5	P_{rx}	0.1 W	A	0.01 m^2
ξ	0.05	ω_1	500	ω_2	800

and the number of PoIs is chosen from $\{5, 10, 15, 20, 15, 30\}$. Since the positions of PoIs are initialized randomly, we run all methods with 40 different initializations and calculate the average result. Note, that a successful K-coverage is attained in each instance. In Figure 3, we report the number of deployed nodes, reliability violations (i.e., the portion of deployed nodes that violate at least one of the reliability bounds) and execution time of each method. The following observations can be made from Figure 3:

- **OPT vs. OPT$_{\mathbf{noRel}}$**. This comparison evaluates the influence of reliability constraints on the optimal solution. Figure 3 shows that OPT deploys 14% more nodes than OPT$_{\mathbf{noRel}}$ to satisfy the reliability constraints. However, if optimizing without the reliability, OPT$_{\mathbf{noRel}}$ will have more 33% - 53% of deployed nodes violating the reliability bounds.
- **R-TSH vs. OPT**. As a heuristic approximating the optimal solution, R-TSH deploys around 20% more nodes than OPT but it is more than 1500x faster. R-TSH always ensures the reliability restrictions.
- **R-TSH vs. TSH, SRIGH**. R-TSH picks 6% and 25% more nodes than TSH and SRIGH, respectively, but does not violate any reliability restrictions. In contrast, TSH and SRIGH have 4% - 8% of violations.
- **Execution Time of OPT and OPT$_{\mathbf{noRel}}$**. The execution time of optimal solvers blows up as we increase the PoIs, which is a consequence of the NP-completeness. Although averaging at around 150 seconds with 25 or 30 PoIs, the execution time can be as poor as 1000 seconds in our experiments. Therefore, it is highly necessary to use heuristics that cost polynomial time in large-scale problems.

2) Large-Scale Problem Simulation: We further conduct a set of simulations in a grid space of 10 km $\times$ 10 km to compare the performances of R-TSH and two heuristic baselines on a larger setting. We configure the coverage level $K = 2$. We report the performances of R-TSH, TSH, and SRIGH, when varying the number of PoIs and the number of grid locations in the field. Similarly, the average result of 40 randomly-initialized cases is shown in Figure 4.

- **Various number of PoIs**. Figure 4a scatters the number of deployed nodes and reliability violations of all heuristics while altering the number of PoIs to be covered. It can be seen that R-TSH places 10% - 20% more nodes than SRIGH but both SRIGH and TSH result in 20% or more reliability violations. Note, that one can explore the trade-off between the number of nodes and reliability

by adjusting reliability bounds SoH_{ref} and $MTTF_{ref}$. Loose reliability constraints will save deployment cost by placing fewer nodes.

- **Various number of candidate locations**. Similar to Figure 4a, Figure 4b depicts the outcomes under various number of candidate locations from 7K to 12K. The reliability violations of TSH and SRIGH fluctuate from 20% to 80% when the size of grid space changes. At the same time, R-TSH consistently keeps the violation rates below 3% while requires 15% - 25% more nodes than SRIGH. Though both using the two-stage mechanism, R-TSH returns much better solutions on the number of deployed nodes and reliability than TSH.
- **Execution Time**. Figure 4c and Figure 4d display the execution time of all heuristics in the above two experiments. R-TSH and TSH consume similar time as they depend on the same mechanism, which is different from SRIGH. When varying the number of PoIs, SRIGH scales linearly in the execution time while R-TSH and TSH take polynomially longer durations. On the other hand, in the experiment of various candidate locations, R-TSH and TSH scale almost linearly while SRIGH lasts polynomially longer. Such difference can be attributed to the node selection procedures.

In summary, R-TSH shows a comparable number of deployed nodes and execution time, while TSH and SRIGH are prone to reliability violations between 20% and 80%.

C. Discussion

1) Impact of External Energy Supply: Unlike [23], the key focus of this paper is on energy-harvesting sensors with rechargeable batteries. Using single-use batteries or rechargeable batteries with external energy supply can cause a huge difference. More concretely, the lifetime of single-use batteries is defined as the time that its state-of-charge (SoC) depletes. SoC is a real number between 0 and 1 suggesting the available charge in comparison to the maximum capacity [13]. While for rechargeable batteries, the state-of-health model is used to predict the operational lifetime, i.e., when SoH reduces to 0.8. We perform a simple experiment to compare the lifetime of using single-use batteries vs. rechargeable ones (Figure 5). Suppose the original capacity of the battery is 1000 mAh and the average current draw is 10 mA. The ambient environment is 30 °C. Using the SoC model in [33] and the SoH model explained in Section III-B, the single-use battery will deplete after approximately 100 days while the rechargeable battery lasts much longer time.

2) Impact of Device Types: The influence of different device types is implicitly integrated into the problem formulation through the conversion from ambient to core temperature (Equation 2). Though not obvious, it largely affects the reliability-driven deployment. We compare the impact of two sets of fitted parameters k_1, k_2, k_3 in Equation 2 obtaining from experiments on low-power MCUs and Raspberry Pis [34] respectively. Based on the temperature conversion model, the equivalent power upper bounds P_{SoH} and P_{MTTF} are derived in order to satisfy given SoH and MTTF constraints at various ambient temperatures (Figure 6). It can be seen that a more powerful platform like Raspberry Pi cannot survive in environments hotter than 30 °C. However, P_{SoH} and P_{MTTF} for low-power MCUs decrease more gently during temperature increment. It is possible for low-power devices to survive in harsh environments if managed properly.

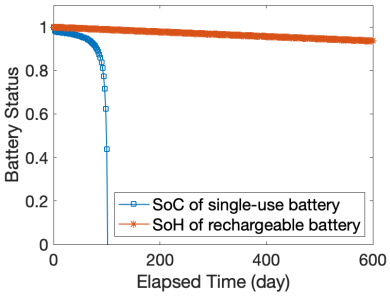

Fig. 5: Compare the fade of state-of-charge for single-use batteries and state-of-health for rechargeable batteries.

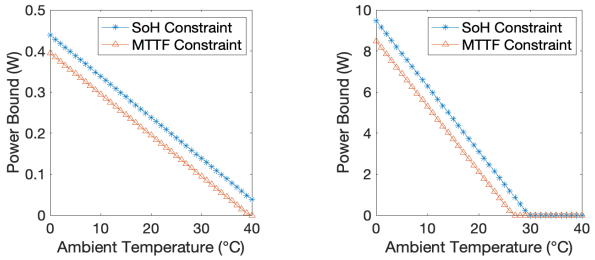

(a) On low-power MCUs. (b) On Raspberry Pis.

Fig. 6: P_{SoH} and P_{MTTF} regarding different devices.

VII. Conclusion

In this paper, we formulate an optimization problem for reliability-driven sensor deployment in energy-harvesting sensor networks. Our goal is minimizing the number of nodes, while guaranteeing: (i) full target coverage, (ii) complete connectivity, (iii) energy-neutral operation, and (iv) reliability constraints. Based on state-of-the-art electronics and battery reliability models, we require two reliability lower bounds to be met after a predetermined time duration. The problem is formulated as MILP and solved with CPLEX. We further propose a greedy heuristic named R-TSH to efficiently find suboptimal solutions in large-scale problems. The simulation results based on a real-world solar irradiance and ambient temperature dataset show that R-TSH meets all reliability constraints with 20% more sensors than the optimal solution while executing more than 1500x faster. R-TSH avoids 20 - 80% of reliability violations with a comparable number of nodes and execution time.

Acknowledgment

This work was partially supported by Semiconductor Research Corporation task #2805.001, and in part by National Science Foundation under Grants #1911095, #1826967, #1730158 and #1527034.

REFERENCES

[1] K. Saravanan, E. G. Julie, and Y. H. Robinson, "Smart cities & iot: evolution of applications, architectures & technologies, present scenarios & future dream," in *Internet of Things and Big Data Analytics for Smart Generation*. Springer, 2019, pp. 135–151.

[2] M. Ayaz, M. Ammad-Uddin, Z. Sharif, A. Mansour, and E.-H. M. Aggoune, "Internet-of-things (iot)-based smart agriculture: Toward making the fields talk," *IEEE Access*, vol. 7, pp. 129 551–129 583, 2019.

[3] Ericsson Mobility Report, "Internet of things forecast," Nov. 2019. [Online]. Available: https://www.ericsson.com/en/mobility-report/internet-of-things-forecast

[4] A. Tripathi, H. P. Gupta, T. Dutta, R. Mishra, K. Shukla, and S. Jit, "Coverage and connectivity in wsns: A survey, research issues and challenges," *IEEE Access*, vol. 6, pp. 26 971–26 992, 2018.

[5] R. Priyadarshi, B. Gupta, and A. Anurag, "Deployment techniques in wireless sensor networks: a survey, classification, challenges, and future research issues," *The Journal of Supercomputing*, pp. 1–41, 2020.

[6] A. Kansal, J. Hsu, S. Zahedi, and M. B. Srivastava, "Power management in energy harvesting sensor networks," *ACM Transactions on Embedded Computing Systems (TECS)*, vol. 6, no. 4, pp. 32–es, 2007.

[7] W. Ejaz and M. Ibnkahla, "Multiband spectrum sensing and resource allocation for iot in cognitive 5g networks," *IEEE Internet of Things Journal*, vol. 5, no. 1, pp. 150–163, 2017.

[8] T. De Schepper, S. Latré, and J. Famaey, "Load balancing and flow management under user mobility in heterogeneous wireless networks," in *2018 14th International Conference on Network and Service Management (CNSM)*. IEEE, 2018, pp. 247–253.

[9] J. Sahoo, M. A. Salahuddin, R. Glitho, H. Elbiaze, and W. Ajib, "A survey on replica server placement algorithms for content delivery networks," *IEEE Communications Surveys & Tutorials*, vol. 19, no. 2, pp. 1002–1026, 2016.

[10] C. Yang and K.-W. Chin, "On nodes placement in energy harvesting wireless sensor networks for coverage and connectivity," *IEEE Transactions on Industrial Informatics*, vol. 13, no. 1, pp. 27–36, 2016.

[11] X. Zhu, J. Li, and M. Zhou, "Optimal deployment of energy-harvesting directional sensor networks for target coverage," *IEEE Systems Journal*, vol. 13, no. 1, pp. 377–388, 2018.

[12] P. Mercati, F. Paterna, A. Bartolini, L. Benini, and T. Š. Rosing, "Warm: Workload-aware reliability management in linux/android," *IEEE Transactions on Computer-Aided Design of Integrated Circuits and Systems*, vol. 36, no. 9, pp. 1557–1570, 2016.

[13] Y. Zou, X. Hu, H. Ma, and S. E. Li, "Combined state of charge and state of health estimation over lithium-ion battery cell cycle lifespan for electric vehicles," *Journal of Power Sources*, vol. 273, pp. 793–803, 2015.

[14] B. Xu, A. Oudalov, A. Ulbig, G. Andersson, and D. S. Kirschen, "Modeling of lithium-ion battery degradation for cell life assessment," *IEEE Transactions on Smart Grid*, vol. 9, no. 2, pp. 1131–1140, 2016.

[15] Cisco Jasper, "The hidden costs of delivering iiot services: Industrial monitoring & heavy equipment," Apr. 2016. [Online]. Available: https://www.cisco.com/c/dam/m/en_ca/never-better/manufacture/pdfs/hidden-costs-of-delivering-iiot-services-white-paper.pdf

[16] "National solar radiation database (nsrdb)." [Online]. Available: https://maps.nrel.gov/nsrdb-viewer/

[17] O. Moh'd Alia and A. Al-Ajouri, "Maximizing wireless sensor network coverage with minimum cost using harmony search algorithm," *IEEE Sensors Journal*, vol. 17, no. 3, pp. 882–896, 2016.

[18] M. Rebai, H. Snoussi, F. Hnaien, L. Khoukhi *et al.*, "Sensor deployment optimization methods to achieve both coverage and connectivity in wireless sensor networks," *Computers & Operations Research*, vol. 59, pp. 11–21, 2015.

[19] M. Elhoseny, A. Tharwat, X. Yuan, and A. E. Hassanien, "Optimizing k-coverage of mobile wsns," *Expert Systems with Applications*, vol. 92, pp. 142–153, 2018.

[20] M. E. Keskin, İ. K. Altınel, N. Aras, and C. Ersoy, "Wireless sensor network lifetime maximization by optimal sensor deployment, activity scheduling, data routing and sink mobility," *Ad Hoc Networks*, vol. 17, pp. 18–36, 2014.

[21] J. Li, W. Liang, M. Huang, and X. Jia, "Providing reliability-aware virtualized network function services for mobile edge computing," in *2019 IEEE 39th International Conference on Distributed Computing Systems (ICDCS)*. IEEE, 2019, pp. 732–741.

[22] S. Harizan and P. Kuila, "Nature-inspired algorithms for k-coverage and m-connectivity problems in wireless sensor networks," in *Design Frameworks for Wireless Networks*. Springer, 2020, pp. 281–301.

[23] X. Yu, K. Ergun, L. Cherkasova, and T. Š. Rosing, "Optimizing sensor deployment and maintenance costs for large-scale environmental monitoring," *To appear in IEEE Transactions on Computer-Aided Design of Integrated Circuits and Systems (TCAD)*, 2020.

[24] T. S. Rosing, K. Mihic, and G. De Micheli, "Power and reliability management of socs," *IEEE Transactions on Very Large Scale Integration (VLSI) Systems*, vol. 15, no. 4, pp. 391–403, 2007.

[25] L. Venkatesan, S. Shanmugavel, C. Subramaniam *et al.*, "A survey on modeling and enhancing reliability of wireless sensor network," *Wireless Sensor Network*, vol. 5, no. 03, p. 41, 2013.

[26] C. Zhuo, D. Sylvester, and D. Blaauw, "Process variation and temperature-aware reliability management," in *2010 Design, Automation & Test in Europe Conference & Exhibition (DATE 2010)*. IEEE, 2010, pp. 580–585.

[27] F. Beneventi, A. Bartolini, A. Tilli, and L. Benini, "An effective gray-box identification procedure for multicore thermal modeling," *IEEE Transactions on Computers*, vol. 63, no. 5, pp. 1097–1110, 2012.

[28] J. Vetter, P. Novák, M. R. Wagner, C. Veit, K.-C. Möller, J. Besenhard, M. Winter, M. Wohlfahrt-Mehrens, C. Vogler, and A. Hammouche, "Ageing mechanisms in lithium-ion batteries," *Journal of power sources*, vol. 147, no. 1-2, pp. 269–281, 2005.

[29] H.-Y. Zhou, D.-Y. Luo, Y. Gao, and D.-C. Zuo, "Modeling of node energy consumption for wireless sensor networks," *Wireless Sensor Network*, vol. 3, no. 1, p. 18, 2011.

[30] M. Abo-Zahhad, M. Farrag, A. Ali, and O. Amin, "An energy consumption model for wireless sensor networks," in *5th International Conference on Energy Aware Computing Systems & Applications*. IEEE, 2015, pp. 1–4.

[31] C. U. Manual, "Ibm ilog cplex optimization studio," *Version*, vol. 12, pp. 1987–2018, 1987.

[32] V. Chvatal, "A greedy heuristic for the set-covering problem," *Mathematics of operations research*, vol. 4, no. 3, pp. 233–235, 1979.

[33] L. M. Rodrigues, C. Montez, R. Moraes, P. Portugal, and F. Vasques, "A temperature-dependent battery model for wireless sensor networks," *Sensors*, vol. 17, no. 2, p. 422, 2017.

[34] "Raspberry pi." [Online]. Available: https://www.raspberrypi.org/